The 2010 IEEE/RSJ International Conference on
Intelligent Robots and Systems
October 18-22, 2010, Taipei, Taiwan

# Detection and measurement of human motion and respiration with microwave Doppler sensor

Hajime Kubo and Taketoshi Mori and Tomomasa Sato

*Abstract*— **A microwave Doppler sensor can monitor human motion without contact. It can sense wide range of motion from minute oscillation like respiration to large movement like walking because it measures the distance change between the target and the sensor as signal phase change. However, the proper method for the signal phase estimation is different between motion and respiration measurement. In this paper, we compare three methods for signal phase estimation and find the optimal method and parameters for each problem. For switching to the proper phase estimation method or monitoring human state, it is important to detect motion signal and respiration signal from the raw signal of sensor output. Three kinds of features, energy, frequency-domain entropy and histogram are extracted and are input into binary classifiers. We tested least squares, SVM and AdaBoost classifiers.**

## I. Introduction

As society is aging, expectation for the automated home monitoring and health care system is growing. To respond sudden diseases or accidents, system is required to observe habitants constantly in their daily life. For daily use, it must not hamper users' activity. Therefore, the devices should sense human unobtrusively.

A microwave Doppler sensor can sense movement without contact, so it does not hamper daily chore. It transmits microwave to the environment and receives the reflected wave. By mixing transmitted signal and received signal, Doppler shift of the microwave reflected from moving object is measured. Then, the change of the range between the sensor and the target is observed as phase change of the output signal. Consequently, the sensor can measure wide range of distance change, from minute oscillation in some millimeters to large motion in meters. As an example of measuring minute oscillation, it has been used for sensing vital signs. Since microwave transmits through clothes and is reflected by the surface of human body, it has been used for contactless remote monitoring of respiration and heartbeat [1], [2], [3]. Meanwhile, as an application of meters of distance change measurement, the position of human target can be estimated with more than three sensors [4], [5].

It can sense wide variety of range change but it cannot measure both large and small distance change simultaneously. Since the output signal of the sensor is one-dimensional time series, the weak signal of minute oscillation is buried in large and high frequency signal of dynamic motion. In fact, there is no way to measure the respiration of a walking target. Moreover, both tiny slow motion and large fast motion can be measured by one sensor, but the good algorithm and its parameters to estimate the velocity of a target from the output signal vary according to the property of the motion. The signal observed while the target is traveling and that while he/she sits still and is breathing are largely different in frequency and strength.

Considering these limitations, it is beneficial to differentiate the observed signals into three categories, one caused by respiration of the target who sits still, one attributed to the target's large movement such as walking or changing posture and the other in which no motion is detected. If these observation states are discerned without the signal phase estimation, we can switch a phase estimating algorithm to a more suitable one according to the situation. Furthermore, this classification is useful for monitoring human state. For example, if no signal state immediately follows the respiration sensing state, it means the cessation of breathing because one cannot go away from the respiration detecting area without moving. There are several related works on measuring both human walk and respiration by a single microwave Doppler radar [6], [7]. They evaluated motion measurement and respiration measurement separately. However, to apply the sensor to monitoring human in daily life, a method to deal with signals in which motion and respiration are mingled is necessary.

In this paper, we study the following two issues. First, we introduce several method for estimating the signal phase and survey which is more suitable for respiration sensing and which is better for motion measurement by comparing them in experiment. Second, we construct three detectors, motion detector, respiration detector and no motion detector for estimating the observation state. Spectral and histogram features are extracted from the raw signal and are processed by binary classifiers.

This paper is organized as follows. First, the output signal and property of the microwave Doppler sensor are formulated in mathematical expression in section II. In section III, three methods for phase estimation are introduced. In section IV, the feature extraction for signal classification is explained. Section V presents the experimental setting and the results. Finally, we conclude in section VI.

## II. Signal model of microwave Doppler sensor

Microwave Doppler sensors are classified into two types, "dual type" and "single type", according to their number of outputs. We use dual type one in this research. It provides two outputs, $V_{IF1}$ and $V_{IF2}$, which have a quadrature phase

H. Kubo, T. Mori and T. Sato are with Graduate School of Information Science and Technology, The University of Tokyo, 7-3-1 Hongo, Bunkyoku, Tokyo, Japan. {kubo, tmori}@ics.t.u-tokyo.ac.jp, tomomasasato@jcom.home.ne.jp

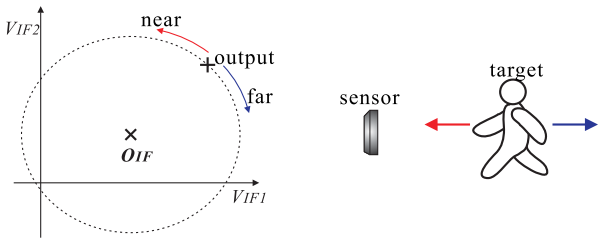


Fig. 1. The signal output point moves on the dotted-line circle, clockwise if the target is going away from the sensor, counterclockwise if the target is coming close to the sensor.

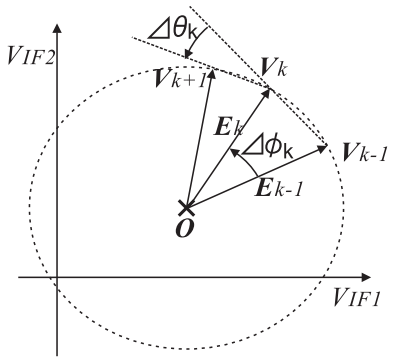


Fig. 2. Vector representation of the signal and phase change. There are two different ways to express signal phase change, $\Delta\phi_k$ and $\Delta\theta_k$.

relationship, that is to say their phases are 90 degrees different from each other. The two outputs are expressed as,

$$V_{IF1} = A_{IF1}\sin(\frac{4\pi R}{\lambda} + \phi_0) + O_{IF1} + w_1 \quad (1)$$

$$V_{IF2} = A_{IF2}\cos(\frac{4\pi R}{\lambda} + \phi_0) + O_{IF2} + w_2 \quad (2)$$

where $A$ is the amplitude of the signal, $\lambda$ is the wave length, $R$ is the distance between the sensor and the target, $\phi_0$ is the initial phase, $O$ is the DC offset and $w$ is the noise. From (1) (2), it is derived that the phase change $\Delta\phi$ is proportional to the range change between the target and the sensor $\Delta R$:

$$\Delta\phi = \frac{4\pi\Delta R}{\lambda}. \quad (3)$$

Thus, signal frequency $f$ is proportional to the velocity of the target:

$$f = \frac{2}{\lambda}v \quad (4)$$

The benefit of "dual type" is that the phase change of the signal can be calculated from the two outputs as explained in following section. This allows the detection of the target's moving direction, whether the target is coming close to or going away from the sensor, while with "single type", one can only calculate the target's unsigned velocity from signal frequency $f$. As illustrated in Fig. 1, the point which indicates the outputs moves around the DC offset point in clockwise or counterclockwise according to the target's moving direction.

Signal amplitude $A$ is monotonic function of received signal power $P_r$,

$$A = CP_r^{\gamma}, \quad (5)$$

where $C$ is a positive constant which depends on gain of peripheral circuit and $\gamma$ is also a positive constant whose value is about 0.5. The received signal power $P_r$ is expressed by radar equation,

$$P_r = \frac{P_t G^2 \lambda^2 \sigma}{(4\pi)^3 R^4} \quad (6)$$

where $P_t$ is the power of the transmitted signal, $G$ is the antenna gain, $\sigma$ is the radar cross section of the target [8]. The antenna gain depends on the radiation pattern and the direction in which the target exists as seen from the antenna. The radar cross section is property of a scattering target. It represents the magnitude of the echo signal which returned from the target to the radar. It depends on the target's size, material and incident angle of the microwave.

## III. Phase Estimation

As expressed in (3), the output signal phase change of the microwave Doppler sensor is proportional to the change of the distance between the target and the sensor. When the two output signals $V_{IF1}$ and $V_{IF2}$ are plotted in a plane as Fig. 1, the signal phase change is expressed as the rotation angle of the output points around the DC offset. A half wave length of distance change corresponds to one revolution as derived from (3).

We calculate the rotation angle of the output as follows. To begin with, we introduce vector representation of the output and the DC offset, $\boldsymbol{V}$, ($\boldsymbol{V} \equiv [V_{IF1}, V_{IF2}]^T$), $\boldsymbol{O}$, ($\boldsymbol{O} \equiv [O_{IF1}, O_{IF2}]^T$). The phase change in a certain period is obtained by accumulating the phase change between samples. The methods to calculate the phase change between samples are divided into two broad categories. The one uses the angle between two consecutive difference vector ($\boldsymbol{V}_{k+1} - \boldsymbol{V}_k$) and ($\boldsymbol{V}_k - \boldsymbol{V}_{k-1}$), which is depicted as $\Delta\theta_k$ in Fig. 2. The merit to use the difference vector is that there is no need for estimating the DC offset. On the negative side, it is vulnerable to noise. Thereafter, DIFF represents this method. The other uses the rotation angle of $\boldsymbol{E}$, a vector from $\boldsymbol{O}$ to $\boldsymbol{V}$. This angle is depicted as $\Delta\phi_k$ in Fig. 2. The angle between two adjacent sample vectors is computed by

$$\Delta\phi_k = \arctan\left(\frac{\boldsymbol{E}_k \times \boldsymbol{E}_{k-1}}{\boldsymbol{E}_k \cdot \boldsymbol{E}_{k-1}}\right). \quad (7)$$

Then the angles are accumulated for the period as,

$$\phi = \sum_{k=0}^{n} \Delta\phi_k, \quad (8)$$

where $n$ is the number of samples contained within the period. These calculations, (7) and (8), are same for the angle between two difference vector in DIFF.

To calculate $\Delta\phi_k$ as above, we have to estimate the DC offset $\boldsymbol{O}$. Since the DC offset fluctuates with several factors such as oscillator power and environmental reflecting condition, the estimation needs to be updated occasionally.

The average over a number of samples is a simple estimate of DC offset in unknown signal. Here we represents this method in capitals, MEAN. However the mean of the output does not correspond to the DC offset when the distance change between the target and the sensor is less than half wave length and the output moves on only a part of the circle. Moreover, if the target stops, samples which have the value at the stop point are obtained more than other points. Consequently, this point is weighted more. Thus, it is considered that MEAN works when the target largely moves but is not suited for slow and minute movement. One more simple approach for estimation of DC offset is linear least squares. This method is derived as follows. First, equalize the amplitudes of the two outputs by multiplying $V_{IF2}$ by $A_{IF1}/A_{IF2}$. Since the ratio $A_{IF1}/A_{IF2}$ is constant, it can be obtained in advance from calibration data which has a good signal to noise ratio. We prepared the calibration data by moving metallic reflection board in front of the sensor. From now on, the output $V_{IF2}$ is assumed to be after this correction so both of the signal amplitudes are described by one variance $A$, as $A_{IF1} = A_{IF2} = A$. Next, we estimate the signal offset $\boldsymbol{O}$ on the following two assumption.

- The offset $\boldsymbol{O}$ is constant in a brief period.
- The distance between the offset $\boldsymbol{O}$ and the output $\boldsymbol{V}$ is constant in this period.

The offset $\boldsymbol{O}$ is calculated from successive $N$ samples. The lengths between offset and all of $N$ outputs are equal to signal amplitude $A$,

$$\|\boldsymbol{V}_i - \boldsymbol{O}\| = A, \tag{9}$$

where $i = 1, \cdots, N$. Then we obtain following by squaring both sides of (9),

$$\|\boldsymbol{V}_i\|^2 - 2\boldsymbol{V}_i^T\boldsymbol{O} + \|\boldsymbol{O}\|^2 = A^2. \tag{10}$$

Subtract two different time samples of (10) and remove quadratic unknown terms, $A^2$ and $\|O\|^2$,

$$2\left(\boldsymbol{V}_i - \boldsymbol{V}_j\right)^T\boldsymbol{O} = \|\boldsymbol{V}_i\|^2 - \|\boldsymbol{V}_j\|^2 \quad (i \neq j). \tag{11}$$

The vector $\boldsymbol{O}$ contains two unknown variables. Thus, if we obtain greater than or equal to two sets of linear equation (11) with more than two samples, $\boldsymbol{O}$ can be estimated by least squares. From here on, we use LS to refer this method. The number of samples $N$ is decided with consideration for the following two conditions. The one is that it has to be small enough to fulfill the assumption that the offset is constant. The other is that the time in which the samples are collected needs to be longer than one cycle of respiration, so that the length of the arc which is formed by the samples is long enough to estimate the center of the circle correctly. The signal amplitude $A$ depends on the relative position and pose between the sensor and the target according to radar equation (6). Therefore the assumption described by (9) is not true when the target is moving around or changing his/her pose. It is anticipated that LS does not work well when the target dynamically moves.

## IV. State detection

The observed microwave Doppler sensor signal is classified into following three states.

*move* The target is changing his/her position or pose.
*resp.* The target sits still and is breathing.
*hold* The target sits still and holds his/her breath.

Three binary classifiers are prepared to detect these three states. Some features are extracted from signal in a certain span and then input to the classifiers.

### A. Feature Extraction

The features are extracted from the samples in a window whose size is $N_w$ samples and which is slid in a step size $N_{step}$ samples. Therefore the feature vector is generated at $Fs/N_{step}$Hz, where $Fs$ is the sampling frequency of the sensor signal. The samples in a window is processed as follows. First subtract the mean of the samples in the window. Then the Fast Fourier Transform (FFT) is performed to obtain spectral features. The first feature signal energy $e$ is calculated as,

$$e = \sum_{n=2}^{N_s} p_n, \tag{12}$$

where $p_n$ is power spectral density (PSD), $N_s$ is number of FFT bins. Next feature, Frequency-domain entropy [9] $H$ is calculated as,

$$H = -\sum_{n=2}^{N_s} \frac{p_n}{e} \log_2\left(\frac{p_n}{e}\right). \tag{13}$$

A peak in spectrum results in low entropy, which means samples contain large monotone signal. Finally, the feature of wave shape is extracted by histogram. The interval between the maximum and the minimum of the samples is divided equally into $N_b$ bins. Therefore the size and the position of bins vary from a window to another window.

In Fig. 3 we give an example of raw signal which contains all three states. The data are sampled at 1kHz. Then from each three state, window size $N_w$ (=4096) of samples are clipped and processed as explained above. This is illustrated in Fig. 4. The energy and entropy features of the samples in Fig. 4 are also listed in table I. The spectrum of *resp.* has a high peak in low frequency, so *resp.* has low frequency-domain entropy. While in *move*, the spectrum peak is not so sharp as in *resp.* because the velocity of the target's movement is not constant. The energy feature is expected to be useful for discerning the nonexistence of motion signal. In fact, the energy of *hold* is obviously smaller than the other two. However, the energy of *move* is not always bigger than that of *resp.* because signal strength largely depends on the relative position and pose between the target and the sensor as described in radar equation (6). The signal wave shape is reflected in the histogram feature. The histogram feature is prone to be monomodal when the signal contains high frequency Doppler signal or has high noise ratio (low S/N). Thus histogram of *move* and *hold* are monomodal in Fig. 4. While low frequency signal has various shape of histogram

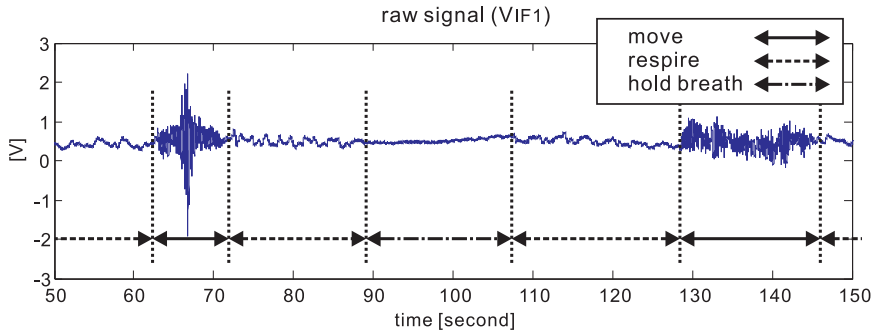


Fig. 3. An example of raw signal which contains all three states, *move*, *resp.* and *hold*

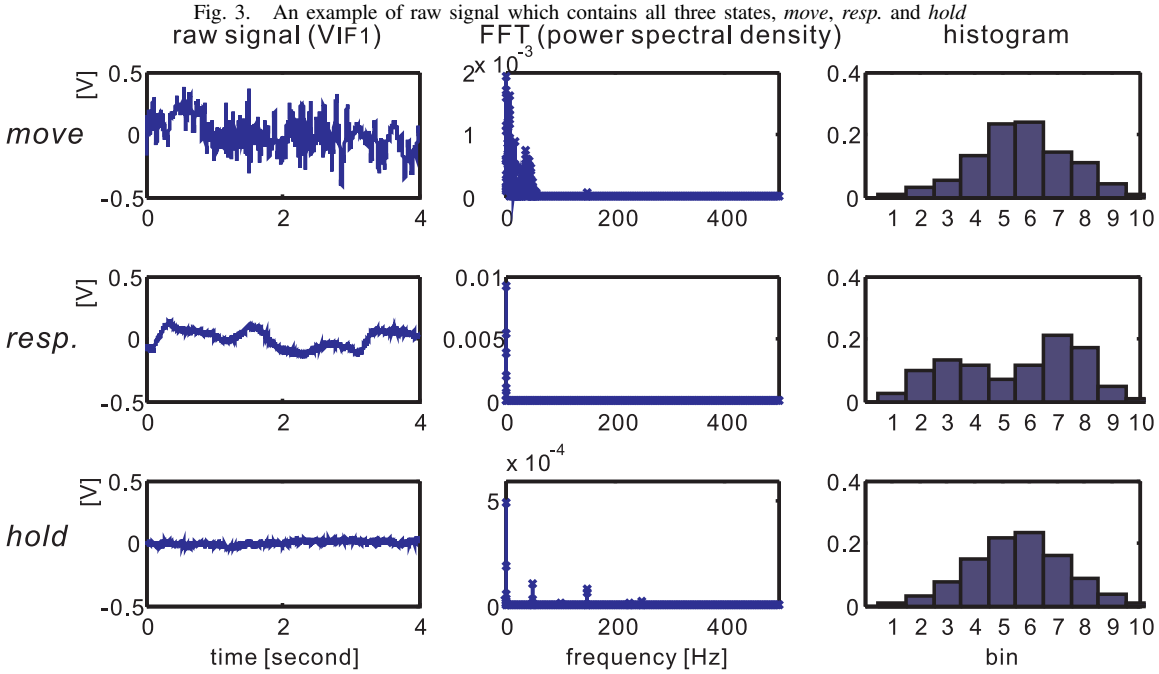


Fig. 4. Clipped raw signals (DC component was removed) and PSDs and histograms in three windows. The target moves in the top row, sits still and respires in the middle row and sits still and holds the breath in the bottom row. PSDs are marked with '×' to distinguish them from x-axis and y-axis.

TABLE I
SIGNAL ENERGY AND FREQUENCY-DOMAIN ENTROPY OF EACH STATE IN FIG. 4

| | move | resp. | hold |
|---|---|---|---|
| energy | 0.056 | 0.023 | 0.0015 |
| entropy | 7.0 | 2.5 | 5.0 |

according to initial phase difference or magnitude of distance change. Especially, since the surface movement of the body involved with respiration stops short between expiration and inspiration and between inspiration and expiration, the samples are accumulate at those two points. Therefore the histogram is likely to be bimodal.

## V. EXPERIMENT

### A. Setup and protocol

*1) hardware:* The microwave Doppler sensor is NJR4261JB0916 (24.11GHz) manufactured by New Japan Radio Co., Ltd. As described in (1) and (2), the sensor signal is summation of Doppler signal which is some tens of millivolts and DC offset which is hundreds of millivolts. Therefore, we need to cut the DC offset before amplifying the Doppler signal. High pass filters do not work because the respiration signal has very low frequency and, in addition, it takes different constant values when the target holds his/her breath after inhaling and after exhaling. Then, we amplified the difference between the sensor output and a constant signal which has roughly same voltage level as the sensor output with an instrumentation amplifier. The constant signal was produced by a voltage divider. The amplified signal is converted into digital form with sampling frequency of 1kHz with NI 6036E which has 16bit differential analog input. The sensor was placed at the height of sitting human's chest, 0.85 meter.

The reference motion and respiration signal was obtained by optical motion capture system *OptiTrack* manufactured by NaturalPoint. The markers were attached both at the microwave Doppler sensor and at the chest of the subject as depicted in Fig.5. The subjects wore an elastic band around

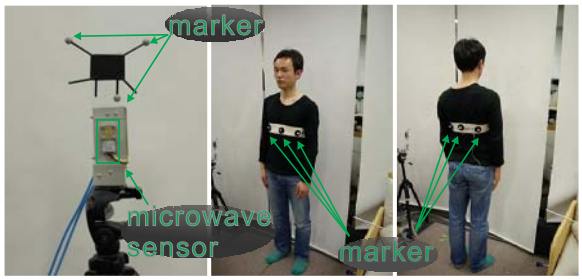


Fig. 5. The sensor and the markers

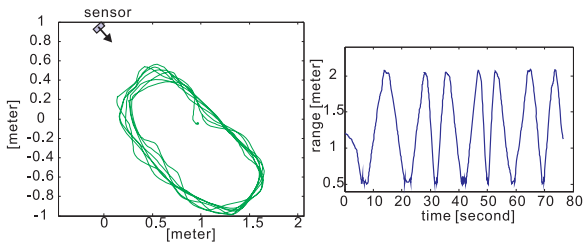


Fig. 6. Left: the trajectory of the target in the motion measurement test. Right: the range between the target and the sensor. Both are obtained by the motion capture.

their chests and six markers were attached on the band. The markers are plastic spheres 16mm in diameter. Their effect on microwave Doppler sensor is negligible in comparison with that of human body surface. Cameras of motion capture were attached at the four corners of the ceiling and at four middle points of each adjacent corners. The dimensions of the room were 5.0 m $\times$ 5.0 m $\times$ 2.4 m (L $\times$ W $\times$ H). The horizontal capture area was about a square 2.5 m on a side at the height of the chest of the target sitting on a chair. The positions of the markers are sampled at 10Hz.

*2) phase estimation:* The phase estimation methods and their parameters were examined to study which is more suited for motion measurement and which is fit for respiration sensing.

First, motion measurement test was done by following way. The subject walked back and forth in front of the sensor in the distance from 0.5 meter to 2.0 meter for 7 rounds in various speed. The trajectory of the target and the range between the target and the sensor in this experiment are shown in Fig. 6. Then the phase was calculated by three methods, MEAN, LS and DIFF. The phase data were linearly interpolated at the sampling time of motion capture data. Then the velocity of the target was calculated both by phase data and motion capture data at the time of motion capture sampling point. The error was calculated as the mean of absolute difference between the velocity measured with microwave Doppler sensor and that obtained from motion capture data. Based on this error, the performance of the phase estimation methods were compared.

Second, data for respiration measurement was obtained as follows. The subject sat still in front of the sensor at the 1.0 to 1.2 meter distance. The subject changed his direction

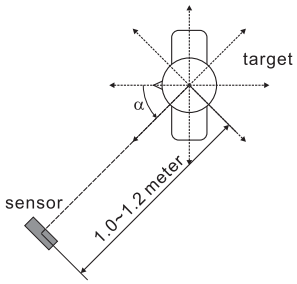


Fig. 7. Respiration measurement was done in eight different directions. The direction of the subject, $\alpha$, was changed from -135 degree to 180 degree in 45 degree step.

TABLE II
THE BODY HEIGHTS AND WEIGHTS OF THE SUBJECTS

| | subject1 | subject2 | subject3 | subject4 |
|---|---|---|---|---|
| height [m] | 1.73 | 1.65 | 1.70 | 1.77 |
| weight [kg] | 62 | 51 | 57 | 65 |

from -135 degree to 180 degree in 45 degree step, where facing to the sensor was 0 degree as shown in Fig. 7. In each pose, subject breathed for about one minute. The data of middle 40 seconds were used for the test. The obtained microwave data were downsampled from 1kHz to 100Hz and low pass filtered with 20Hz cutoff frequency. The reference data were the distance between the sensor and the marker nearest to the sensor of the six markers attached to the subject. The sample point of motion capture and microwave was synchronized by interpolation in the same manner as for the motion measurement test. Based on the correlation coefficient between the reference range change and the estimated phase change, the performance of the phase estimation methods are compared.

*3) state detection:* In this experiment, four subjects volunteered. All are males and range in age from 23 to 29. The body heights and weights of the subjects are described in Table II. Three chairs are arranged in front of the sensor as illustrated in Fig.8. The subjects sat on the each three chairs sequentially as following protocol.

$i = j = 1$;
**WHILE** $j < 5$
Sit still on the $chair(i)$ facing $direction(j)$.
Breathe about 8 to 10 cycle.
Hold breath for about 10 seconds.
Breathe about 8 to 10 cycle.
**IF** $i == 3$ **THEN** $i = 1$, $j = j + 1$
**ELSE** $i = i + 1$
**ENDIF**
Move to $chair(i)$.
**ENDWHILE**

where $direction(j)$ $(j = 1, \cdots, 4)$ are four directions depicted by arrows in Fig. 8. The subjects moved between three positions four rounds.

The obtained raw data were processed into dataset. First the motion capture data were labeled as *move*, *resp.* and *hold*

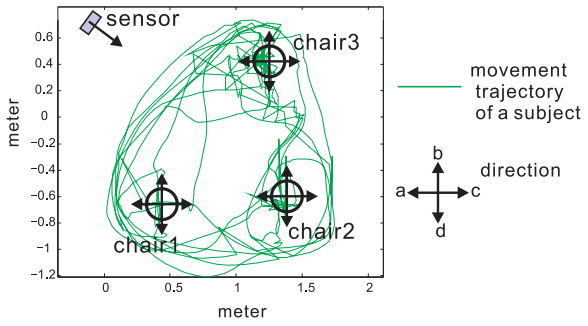


Fig. 8. The sensor and the target position of detection experiment.

by following way.

*hold* more than five seconds period in which the magnitude of movement of the markers attached to the subject is less than 0.003 meter

*resp.* more than ten seconds period other than *hold* in which the magnitude of movement of the markers attached to the subject is less than 0.025 meter

*move* other period

After this labeling, we modified obviously wrong labels by hand, referring to the protocol. The parameters in feature extraction were, window size: $N_w = 4096$, step size: $N_{step} = 1000$, number of bins: $N_{bin} = 10$. In total 3394 samples were prepared, 447 *move*, 2266 *resp.* and 681 *hold*.

Following three kinds of binary classifiers were tested.

- Simple linear least-squares classifier (LS).
- Support Vector Machine (SVM).
- AdaBoost classifier

We used libSVM by Chang et al. [10] for computation of SVM and GML AdaBoost Toolbox by A. Vezhnevets[11] for AdaBoost training. We chose decision stump for weak learner of AdaBoost.

To evaluate the performance of each detector, four-fold cross validation test was done. The data were divided into four sets in two different ways. One is dividing data by rounds, in which both training and test data contains data of all the subjects. The other is dividing data by subjects. Therefore training data do not contain the data which belong to the subject of test data.

### B. Result

*1) phase estimation:* As shown in table III, MEAN showed the best performance of the three methods for motion measurement. It is suited for the high frequency signal. In using the method MEAN or LS, the window size need to be decided properly. We searched the proper size by testing window size from 10 to 1,000 samples with 10 samples increments in between, as shown in Fig.9-C. Both MEAN and LS showed best performance at window size of 30 samples.

In respiration measurement, we cannot see the respiration wave by DIFF because error larger than respiration signal is accumulated as shown in the top figure of Fig. 12. Thus MEAN and LS are compared. Window size test was also

TABLE III
ERROR IN MOTION ESTIMATION

| | MEAN | LS | DIFF |
|---|---|---|---|
| error [m/s] | 0.10 | 0.11 | 0.14 |

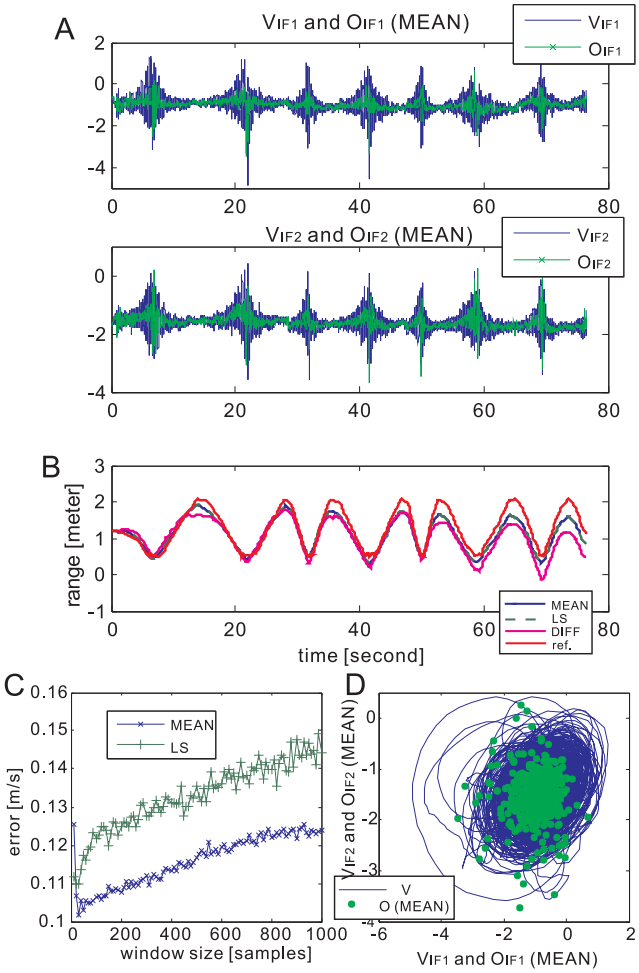


Fig. 9. Phase estimation result in *move*. A and D: raw signals and estimated dc offset (MEAN $N_w = 30$). B: Estimated phase (MEAN, LS and DIFF. Window sizes of MEAN and LS are both 30 samples.) and reference are compared. C: Window size test

done in respiration monitoring. As seen from Fig. 10, four seconds window size is suited for respiration sensing. This length, four seconds, is close to the respiration period. LS is little better than MEAN, especially in the case that there is large angle between the sensor direction and the subject direction.

As an example, the signals, the estimation and the evaluation of the respiration measurement in which the direction of the target was 45 degree are shown in Fig. 11 and Fig. 12. The raw signals and offset estimation are shown in Fig. 11. These indicate the necessity of occasional update for the DC offset estimation. The range between the sensor and the human chest surface and its derivative, that is to say velocity, were calculated from the signals in Fig. 11. They are shown

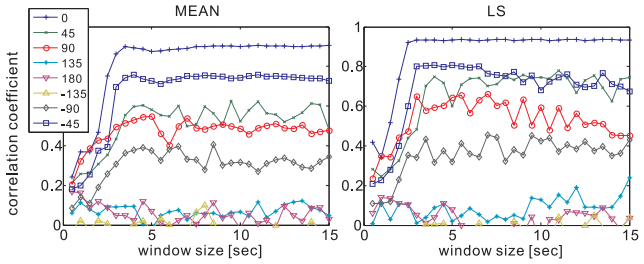


Fig. 10. The effect of the window size on respiration measurement. The measurement performance was evaluated according to correlation coefficient between the reference and the estimated phase change.

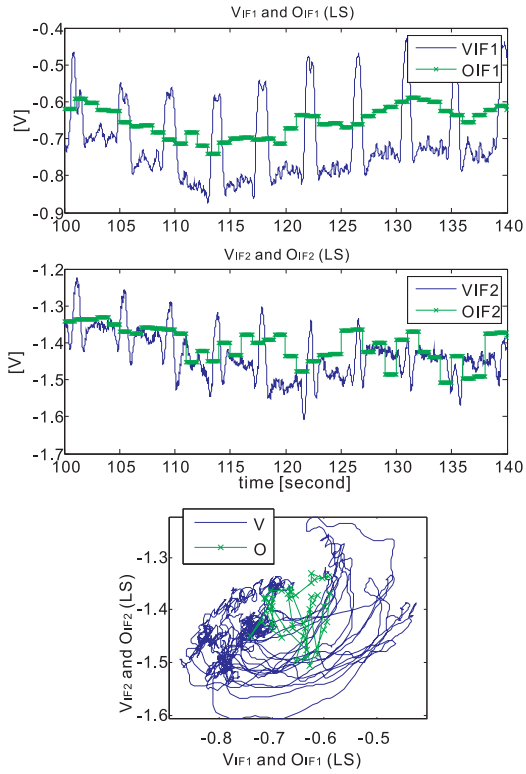


Fig. 11. An example of raw signals of the microwave Doppler sensor and the estimation of their DC offsets in respiration measurement. The DC offsets are estimated by LS whose window size is four second.

in Fig. 12. Since we cannot measure the absolute range with a microwave Doppler sensor, the estimated ranges at 100 second are conformed to the reference for the facility of comparing their wave shapes with that of the reference.

The results of these two experiments show that the appropriate sampling frequency, algorithm, and window size for the measurement of the motion and the respiration are totally different.

*2) state detection:* The receiver operating characteristic (ROC) curves of each detector were obtained by testing their performance with different thresholds. The results are shown in Fig. 13, where $P_D$ is probability of detection and $P_{FA}$ is probability of false alarm. The performance difference between classification methods are little. Motion detection was done well and detecting *hold* was poor in

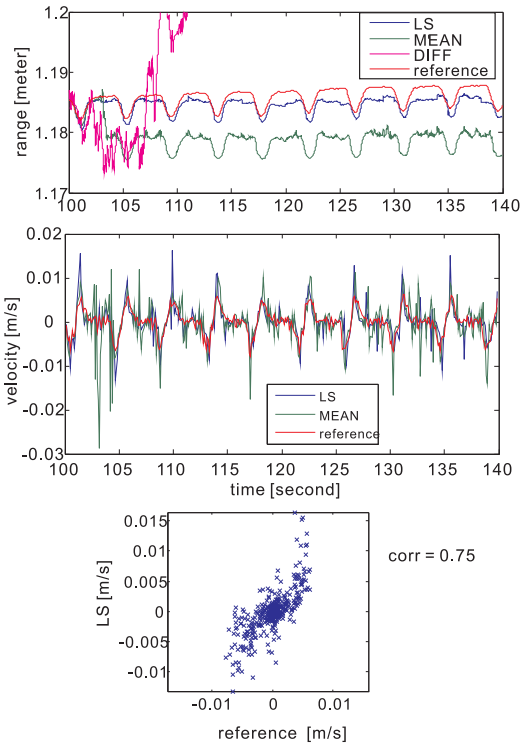


Fig. 12. Top: respiration wave shape estimated from the signals in Fig. 11 compared with reference. Middle: estimated velocity compared with reference velocity. Bottom: correlation between estimated velocity (LS) and reference velocity.

all classifiers. The performance tested by cross validation whose data division was done by subjects is not worse than that tested by round based division. This means that the state detection does not depend on the individual target. The parameters can be configured at the factory.

The effects of each feature on detection were tested by changing the features which were used for the detection. The classifier was AdaBoost and the data were divided by round. The results are shown in Fig. 14. The energy is important for the detection of *move* while the entropy is useful for the detection of *resp.* All detectors work best when all the three kinds of features are used.

## VI. Conclusion

We studied two topics in this paper, phase estimation and state detection of the output signal of a microwave Doppler sensor. To calculate the signal phase, DC offset of the signal needs to be estimated in advance. The proper method for offset and phase estimation is different for the velocity and magnitude of the target motion. We proposed three methods, DIFF, LS and MEAN. Result of our experiment showed that, in the proposed three methods, the simple average of the samples, MEAN, was the best of the three when the target is walking. The linear least squares estimation, LS, was the best in sensing the respiration of the target at rest. The proper window size was 30 samples at 1kHz for movement measurement and 400 samples at 100Hz for respiration measurement. In the detection problem, three states *move*, *resp.* and *hold*

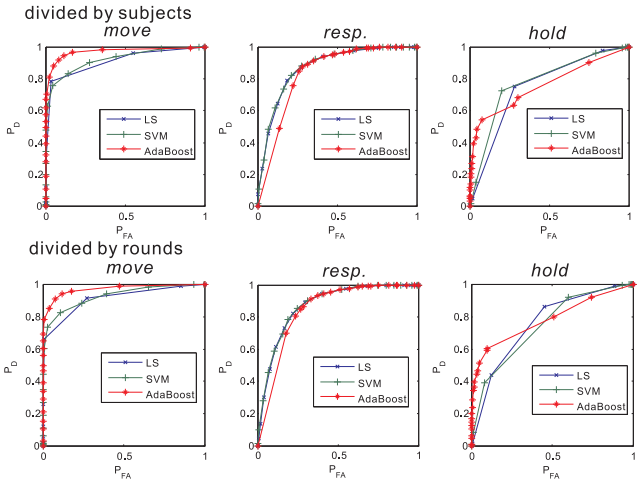


Fig. 13. ROC curve of *move*, *resp.* and *hold* detector. Detection test was done with four-fold cross validation. Data were divided by subjects (first row) or by rounds (second row).

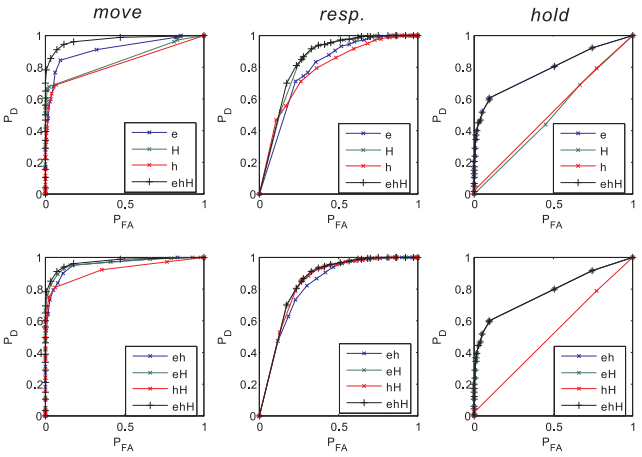


Fig. 14. The effects of each feature on detection. The characters in legends denote the features which are used for the detection, where 'e': energy, 'H': entropy, 'h': histograms.

were detected by three binary classifiers prepared for each state. For input of the classifiers, the energy, frequency-domain entropy, and histogram features were extracted from raw signal. We tested three methods, least squares, SVM and AdaBoost for binary classification. The result of the experiment showed that there is no significant difference between the performance of classification methods. Cross validation was done by two different ways of data division. One is dividing the data by the rounds of data acquisition protocol. The other is dividing the data by the subjects. As a result, the classifiers trained by other person's data was not inferior to those trained by data which contain the target's own data.

There are some problems to be solved in the future work. In this paper, all experiments and evaluation are done under the assumption that the target exists in the detection and measurement area of the sensor. However, it is important to decide whether the target is in the area or not from

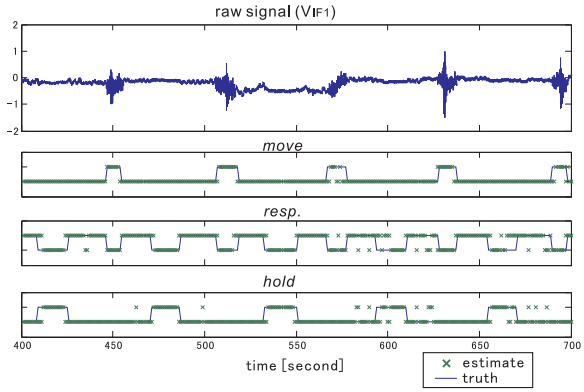


Fig. 15. An example of state detection. Signals of one subject are tested by classifier trained by data of the other three subjects. The AdaBoost classifier is used.

the observed signal and time series of the detection result. The signal strength depends on the relative position and pose between the target and the sensor. This dependency of measurability on the position and pose has not yet been defined.

## REFERENCES


[1] E. F. Greneker, "Radar sensing of heartbeat and respiration at a distance with applications of the technology," in *Radar*, 1997, pp. 150–154.

[2] A. Droitcour, V. Lubecke, J. Lin, and O. Boric-Lubecke, "A microwave radio for Doppler radar sensing of vital signs," in *Microwave Symposium Digest, 2001 IEEE MTT-S International*, vol. 1, 2001, pp. 175 – 178.

[3] D. R. Morgan and M. G. Zierdt, "Novel signal processing techniques for Doppler radar cardiopulmonary sensing," *Signal Processing*, vol. 89, pp. 45–66, 2009.

[4] B. Kusy, L. A., and K. X., "Tracking mobile nodes using rf Doppler shifts," in *5th ACM International Conference on Embedded Networked Sensor Systems (Sensys)*, 2007.

[5] H. Kubo, T. Mori, and T. Sato, "Human location estimation with multiple microwave Doppler sensors in home environment," in *Sixth International Conference on Networked Sensing Systems*, 2009, pp. 39 – 44.

[6] M. Zakrzewski, A. Kolinummi, and J. Vanhala, "Contactless and unobtrusive measurement of heart rate in home environment," in *28th Annual International Conference of the IEEE EMBS*, 2006, pp. 2060 – 2063.

[7] B.-K. Park, V. Lubecke, O. Boric-Lubecke, and A. Host-Madsen, "Center tracking quadrature demodulation for a Doppler radar motion detector," in *Microwave Symposium, 2007. IEEE/MTT-S International*, 2007, pp. 1323–1326.

[8] M. I. Skolnik, *Introduction to radar systems*, 3rd ed. McGRAW-HILL, 2001.

[9] L. Bao and S. S. Intille, "Activity recognition from user-annotated acceleration data," *PERVASIVE*, pp. 1– 17, 2004.

[10] C.-C. Chang and C.-J. Lin, *LIBSVM: a library for support vector machines*, 2001, software available at http://www.csie.ntu.edu.tw/ cjlin/libsvm.

[11] A. Vezhnevets, MSU Graphics & Media Lab, Computer Vision Group, http://graphics.cs.msu.ru.